Desalination and Water Treatment
www.deswater.com

doi: 10.1080/19443994.2015.1119754

57 (2016) 21598–21609
September

Taylor & Francis
Taylor & Francis Group

Cr *K*-edge X-ray absorption and FTIR spectroscopic study on the reaction mechanisms of Cr(III) and Cr(VI) with lignin

Yu-Chi Lin[a], Shan-Li Wang[b,*]

[a]*Department of Soil and Environmental Sciences, National Chung Hsing University, Taichung 40227, Taiwan, email: ivy20p@hotmail.com*
[b]*Department of Agricultural Chemistry, National Taiwan University, Taipei 10617, Taiwan, Tel. +886 233664808; Fax: +886 223660751; email: wangsl@ntu.edu.tw*

Received 17 June 2015; Accepted 24 October 2015

ABSTRACT

The reaction mechanisms of lignin with Cr(III) and Cr(VI) were investigated using Cr *K*-edge X-ray spectroscopy (XAS) and FTIR spectroscopy. The spectroscopic results for lignin reacted with Cr(III) showed that the adsorbed Cr(III) has a coordination environment similar to that of $Cr(H_2O)_6^{3+}$ ion, and the carbonyl groups of lignin are predominately responsible for adsorbing Cr(III). Accordingly, the reaction mechanism of Cr(III) with lignin was determined to be surface adsorption through the formation of an outer-sphere complex. In contrast, Cr(VI) reaction with lignin is not simply surface adsorption. Upon reaction with lignin, Cr(VI) was reduced to Cr(III), which was either bound to lignin or released back into solution. The corresponding FTIR spectra revealed that the carbonyl and phenolic groups are the primary sites for reducing Cr(VI) to Cr(III), leading to the formation of carboxyl groups. The carboxyl groups chelate Cr(III) to form a bidentate inner-sphere complex, deduced from the XAS and FTIR results. The formation of polynuclear Cr(III) species on the lignin surface after Cr(VI) reaction was also detected. The results of this study provide new insights into the reaction mechanisms of Cr(III) and Cr(VI) with lignin, and these new insights can be used to re-evaluate the results of macroscopic observations in the literature.

Keywords: Lignin; Hexavalent chromium; Reduction; Trivalent chromium; Adsorption; Reaction mechanism

1. Introduction

Cr is one of the most frequently found pollutants in the environment because of its extensive uses in various industries, such as metal finishing and leather tanning [1,2]. The effluents from these industries contain Cr(VI), Cr(III), or both [1,2]. Minimization of the environmental risk of toxic Cr necessitates the development of methods for removing Cr from industrial effluents and polluted water; thus, a wide variety of materials have been tested for their Cr removal efficacies [3–5]. Among the tested materials with a promising Cr removal capacity, lignocellulose-based agricultural wastes have received considerable attention because their high abundance and low cost are beneficial for developing cost-effective methods for large-scale treatment of Cr-containing waters [4,5]. As summarized by Miretzky and Cirelli [4], lignocellulosic materials exhibited removal capacities for Cr(III)

*Corresponding author.

and Cr(IV) as high as 38 and 286 mg g^{-1}, respectively, depending on the reaction time, reaction temperature and material dosage, and on the pH, ionic strength, and presence of co-existing chemical species in the water being treated. Nonetheless, the number of studies of Cr removal by new lignocellulosic materials in the literature continuously increases, and the reaction mechanisms reported on the basis of macroscopic measurements are often controversial [5,6]. This controversy reflects the fact that we have not acquired sufficient knowledge about the Cr reaction mechanisms of lignocellulosic materials. Thus, the predominant constituents of the materials and the reaction mechanisms involved in Cr removal need to be clearly elucidated. Moreover, after a lignocellulosic material has been used to treat Cr-containing water, ultimate disposal or recovery of Cr retained by the used materials is important for lowering the overall environmental risk of Cr pollution [7,8]. An understanding of the structural properties of Cr retained by the used materials is necessary for the proper treatment of the materials to prevent secondary pollution of Cr released from the materials.

The goal of this study was to investigate the reaction mechanisms of Cr(III) and Cr(VI) with lignin and the structure of Cr retained on lignin after the reactions. Lignin, which is the second-most abundant component of lignocellulose after cellulose, consists of cross-linked monolignols, primarily *p*-hydroxyphenyl, guaiacyl, and syringyl units [9]. These units contain various functional groups, including methoxyl, phenolic hydroxyl, benzyl alcohol, and carbonyl groups, which play a key role in determining the surface reactivity of lignin toward organic and inorganic pollutants [10–12]. Lignin has been suggested to predominately determine the overall reactions of lignocellulosic materials with Cr(III) and Cr(VI) [4,13], although cellulose and hemicellulose can also contribute to a level of relative significance [14,15]. Lignin can be obtained in large quantities as waste from paper mills and can potentially be used as a low-cost adsorbent for removing Cr(III) and Cr(VI) from wastewaters [11,12]. Various studies on the reactions of Cr(III) and Cr(VI) with lignin have been performed using macroscopic experimental methods and adsorption models [16–19]. Lignin exhibits adsorption capacities toward both Cr(III) and Cr(VI), which is attributed to the electrostatic attraction of these ions to negatively and positively charged functional groups of lignin, respectively [16,17]. However, macroscopic studies cannot provide information about the bonding structure of Cr adsorbed onto lignin after Cr(III) and Cr(VI) reactions; thus, the reaction mechanisms of Cr(III) and Cr(VI) with lignin remain subject to debate. Microscopic studies are therefore required for achieving mechanic understanding of the reactions of Cr(III) and Cr(VI) with lignin.

In this study, FTIR and Cr *K*-edge X-ray spectroscopy (XAS) were used to investigate the structure of Cr bound to lignin after the reactions of Cr(III) and Cr(VI) and the functional groups of lignin responsible for the reactions. The XAS of an absorbing element, arising from the transitions of excited electrons to unoccupied electronic levels, can provide microscopic information regarding the coordination geometry of the element to ligands [20]. XAS was therefore suitable for determining the bonding structure of Cr bound to the functional groups of lignin after Cr(III) and Cr(VI) reactions. FTIR spectroscopy is very sensitive to changes in the composition of functional groups in materials and in the binding modes of specific functional groups toward metal ions; thus, it was used to identify the functional groups of lignin that react with Cr(III) and Cr(VI). The complementary information from these spectroscopic methods was further analyzed to provide insights into the mechanisms by which Cr(III) and Cr(VI) react with lignin. This knowledge can serve as the basis for re-interpreting the results of macroscopic studies reported in the literature and can advance our understanding of the Cr reactivity of lignocellulosic materials, thereby facilitating the development of cost-effective methods for treating Cr-polluted water.

2. Materials and methods

2.1. Reactions of Cr(III) and Cr(VI)

Lignin (0.05 g) was placed in each of a series of 50-mL amber glass centrifuge tubes with Teflon-lined caps, and 25 mL of Cr solution was subsequently added to each tube. The stock solutions of 100 mg L^{-1} Cr(III) and 1,000 mg L^{-1} Cr(VI) were prepared by dissolving 0.256 g $CrCl_3{\cdot}6H_2O$ and 3.734 g of K_2CrO_4, respectively, in 500 mL of 0.01 M KCl solution at pH 2. These solutions were subsequently used to prepare the working solutions in the experiments. The initial concentrations of Cr(III) and Cr(VI) ranged from 1 to 50 mg L^{-1} and from 20 to 1,000 mg L^{-1}, respectively. Samples for each Cr concentration were prepared in triplicate. After 72 h of reaction, the suspensions in the tubes were filtered through a 0.2-μm cellulose acetate membrane filter to collect the filtrates and solids. The solids were washed with deionized water to remove residual Cr, freeze-dried, and stored in plastic bottles prior to further spectroscopic analyses. The total Cr concentration in the filtrates was determined using ICP-AES; the difference between the total Cr

concentrations before and after reaction was attributed to the amount of Cr adsorbed onto lignin (Eq. (1)). In the Cr(VI) reaction experiments, the Cr(VI) concentration in the filtrates was determined using the colorimetric diphenylcarbohydrazide (DPC) method at 540 nm [21], and the difference between the total Cr and Cr(VI) concentrations in solution was attributed to the Cr(III) concentration in solution. The amount of Cr(VI) removed by lignin from solution was calculated using Eq. (2):

$$\text{Cr adsorbed on lignin}\,(\text{mg g}^{-1}) = \left(C_{\text{i,total Cr}} - C_{\text{r,total Cr}}\right)/s \quad (1)$$

$$\text{Cr(VI) removed by lignin}\,(\text{mg g}^{-1}) = \left(C_{\text{i,Cr(VI)}} - C_{\text{r,Cr(VI)}}\right)/s \quad (2)$$

where C_i and C_r are the initial and residual concentrations of total Cr or Cr(VI) in units of mg L^{-1} and s is the solids concentration (i.e. 2 g L^{-1}).

2.2. Cr K-edge XAS

The Cr *K*-edge XAS measurements were conducted at Beamline 17C at the National Synchrotron Radiation Research Center in Hsinchu, Taiwan. The beamline optics includes a vertically collimating pre-mirror, a fixed-exit double-crystal Si (111) monochromator, and a toroidal focusing mirror. The XAS spectra of samples were collected in fluorescence mode using a Lytle detector with a 6-μm vanadium filter and a set of Soller slits. At least three scans were collected for each sample, and the spectrum of a metallic Cr film was simultaneously collected in each scan for energy calibration to 5,989 eV (i.e. E_0). The different scans of each sample were then averaged. Cr *K*-edge XAS measurements were also conducted for selected reference compounds, including Cr(III) acetate hydroxide (CrAH, $Cr_3(OH)_2(CH_3CO_2)_7$), Cr(III) acetylacetonate (CrAA, $Cr(C_5H_8O_2)_3$), $Cr(OH)_3$, and CrO_3. These reference compounds were diluted in cellulose to yield a Cr concentration of 1 mg g^{-1} prior to the Cr *K*-edge XAS measurements. A 1 g L^{-1} solution of $Cr(H_2O)_6^{3+}$ was prepared by dissolving $Cr(NO_3)_3$ in deionized water at pH 1 and was subsequently analyzed using XAS. The oxidation state and coordination environment of Cr remained unchanged during the measurement of any sample or reference compound, as observed in multiple scans.

Spectral processing and analysis were conducted using the Athena program [22] according to the procedure suggested by Kelly et al. [23]. For each XAS spectrum, the pre-edge and post-edge regions were set to 0 and 1, respectively. The E–E_0 region from −10 to 50 eV in each normalized spectrum was then isolated for X-ray near-edge structure (XANES) analysis. For selected samples, the extended X-ray absorption fine structure (EXAFS) data were extracted from the corresponding XAS spectra using the Autobk algorithm implemented in the Athena program and then converted to photoelectron wave vector units (i.e. $\chi(k)$ with a unit of Å^{-1}). The k^3-weighted $\chi(k)$ function was Fourier transformed over a k-range of ~3.7–13.4 Å^{-1} with the Hanning window (dk = 1). The resulting Fourier transform (FT) magnitude in the region of 1–3 Å was fitted using the Artemis program [22] with the theoretical parameters of selected scattering paths, which were generated using Feff 8.2 [24] with the structural parameters of α-CrOOH [25] and basic chromium acetate [26]. The amplitude reduction function (S_0^2) was constrained to a value of 0.85, which was obtained by fitting the experimental spectrum of Cr $(OH)_3$. Fitted parameters included the coordination number (CN), interatomic distance (R), Fermi shift (ΔE_0), and Debye–Waller factor (σ^2). The k^1-, k^2-, and k^3-weighted FT magnitudes were fitted simultaneously to decouple the correlations between the parameter pairs [27]. Although the FT magnitudes of some samples exhibited spectral features in the region > 3 Å, fitting these features with a combination of single and multiple-scattering paths cannot provide a unique solution. Thus, no attempt was made to fit the spectral features in the region > 3 Å.

Structural parameters for Cr adsorbed onto lignin after Cr(III) or Cr(VI) reaction were obtained using the following spectral fitting procedure in an iterative manner. The CN of O atoms in the first shell around Cr was set to 6, and initial guesses were entered for R, ΔE_0, and σ^2. After the fit of the Cr–O path converged, the parameters of either Cr–C or Cr–Cr paths were then added to account for the presence of C or Cr in the second shell around Cr. To reduce the number of free parameters, one ΔE_0 value was used for all scattering paths. The CN values of C and Cr were initially assigned to a potential integral value according to the amplitude of the residuals and were then allowed to vary only at the final fitting step. After a ΔE_0 value was obtained, the R or σ^2 factors were then allowed to float. This process was reiterated until the value of the error parameter $\varepsilon = \sum(\chi_{\text{exp}} - \chi_{\text{fit}})^2 / \sum(\chi_{\text{exp}})^2 < 0.001$, where χ_{exp} and χ_{fit} are the experimental and calculated $\chi(k)$ functions, respectively. If an optimized fit could not be obtained for a model containing either the Cr–C or the Cr–Cr path, both scattering paths were then included in the model to fit EXAFS spectra. In this case, the parameters of the Cr–C path were added

after all the parameters of the Cr–O and Cr–Cr paths converged. This was because the spectral contribution from the Cr–C path is relatively small. While the parameters of the Cr–C path were fitted, the parameters of the other paths were held constant. After the parameters of the Cr–C path converged, the whole fitting process was reiterated until the variation in each parameter was small and the calculated value of the error parameter $\varepsilon < 0.001$.

2.3. FTIR spectroscopy

Transmission FTIR spectra were acquired for the lignin samples before and after the reaction with Cr(III) or Cr(VI) using a Thermo Nicolet Nexus FTIR spectrometer, which was equipped with a KBr beamsplitter and an MCT detector. The samples were randomly distributed in a KBr pellet with a sample/KBr ratio of 1:200 (w/w). Spectra in the range of 2,000–600 cm^{-1} (i.e. the fingerprint region) were obtained by co-addition of 128 individual scans with an optical resolution of 4 cm^{-1}. The IR spectra were plotted and analyzed using the Grams AI® program (Thermo Scientific).

3. Results and discussion

3.1. Cr(III) reaction mechanism

Fig. 1 shows the amount of Cr(III) adsorbed onto lignin as a function of the initial Cr(III) concentration. The experiment was conducted at pH 2, where the predominant species of Cr(III) is $Cr(H_2O)_6^{3+}$ [28]. Thus, hydrolytic species or precipitates of Cr(III) did not interfere with the spectroscopic investigation of the structure of adsorbed Cr(III) ions. As shown in Fig. 1, the Cr(III) adsorption isotherm is of the L-type [29]. To further clarify the adsorption mechanism of Cr(III), samples S1–S4 were selected for XAS and FTIR spectroscopic analyses.

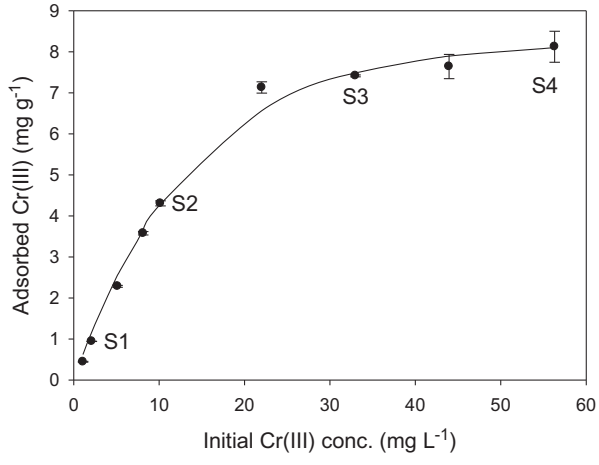

Fig. 1. Cr(III) adsorption of lignin as a function of the initial Cr(III) concentration at pH 2.

3.1.1. Cr K-edge XAS

In Fig. 2, the XANES spectra of samples S1–S4 are compared with those of Cr(III)-containing reference compounds. These XANES spectra all exhibited weak pre-edge features, a strong main absorption edge (i.e. the white line) and post-edge features on the high-energy end of the white line. These spectral features are sensitive to the coordination environment of Cr, as revealed by the significant differences in the XANES spectra of the reference compounds. As shown in Fig. 2, the XANES spectra of samples S1–S4 all match well with that of $Cr(H_2O)_6^{3+}$ in solution (red dashed lines). This similarity suggests that the coordination environment of Cr(III) adsorbed on lignin at different Cr(III) concentrations exclusively resembles that of $Cr(H_2O)_6^{3+}$ in solution. Therefore, the coordination

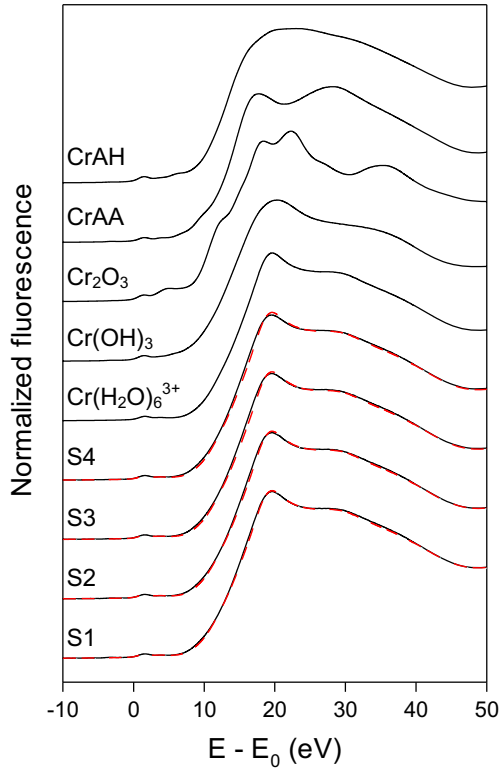

Fig. 2. Cr *K*-edge XANES spectra for Cr(III)-containing reference compounds and lignin samples collected after the reaction of Cr(III) at different concentrations (samples S1–S4 are indicated in Fig. 1).

geometry of the inner hydration shell around Cr^{3+} in adsorbed Cr(III) is not significantly altered upon binding to the surface of lignin. That is, the functional groups of lignin do not directly chelate the central Cr^{3+} ion in Cr(III) adsorbed on lignin; thus, the adsorbed Cr(III) forms an outer-sphere complex on the lignin surface.

Because the XANES spectra of the samples were independent of the amount of Cr(III) adsorbed, only the EXAFS spectrum of the sample with the maximal Cr adsorption (i.e. S4 in Fig. 1) was fitted using the theoretical parameters from Feff to determine the type, number, and distance of neighboring atoms around the central Cr^{3+} in the adsorbed Cr(III). The experimental and fitted FT magnitudes of the EXAFS spectrum are shown in Fig. 3. The CN and Cr–O distance (R) of O in the first shell around Cr were determined to be 6 and 1.99 Å, respectively (Table 1), which are consistent with the octahedral coordination environment reported for hydrated Cr^{3+} ions [30–32]. Although the scattering path of the C or Cr in the second shell was included to fit the EXAFS spectrum, no acceptable fit could be obtained for either path. These results therefore indicated that neither C nor Cr was present in the second shell of the adsorbed Cr(III) on lignin. In the absence of neighboring Cr, the occurrence of polynuclear Cr species or Cr-hydroxide precipitates on the surface of lignin was ruled out. Thus, the adsorbed Cr(III) was present as a monomer bound to lignin. The absence of neighboring C in the second shell of Cr revealed that the central Cr^{3+} ion of the adsorbed Cr(III) was not directly bound to the functional groups of lignin, consistent with the corresponding XANES spectrum. In other words, the oxygen atoms in the first coordination shell of the adsorbed Cr(III) on lignin were exclusively contributed by hydration water molecules or hydroxyl ions. Therefore, the Cr(III) adsorption mechanism of lignin is the formation of outer-sphere complexes, and electrostatic interaction and/or H-bonding is involved in the interaction between the adsorbate and adsorbent. In this case, the O and C of the functional groups of lignin are present in the coordination shells beyond the first hydration shell of Cr^{3+} in the adsorbed Cr(III) species. Their spectral contributions are overlapped with those of the first-shell multiple-scattering (MS) path and the scattering paths of the higher shells, such as water molecules and counterions. Consequently, EXAFS does not permit us to identify the functional groups that form outer-sphere complexes with Cr(III) adsorbed on lignin.

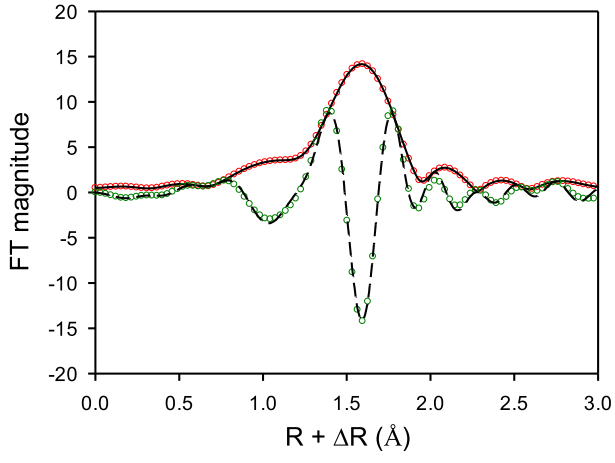

Fig. 3. Fourier transform magnitude of the K-edge EXAFS for Cr(III) adsorbed on lignin at pH 2 (solid line) and the corresponding imaginary part (dashed line). The open circles and line represent the experimental and fitted data, respectively.

3.1.2. FTIR spectroscopy

The FTIR spectra of lignin before and after Cr(III) reaction were examined to identify the binding sites for the adsorbed Cr(III) species (Fig. 4). The FTIR spectrum of the original lignin showed bands at 1,710, 1,597, 1,512, 1,462, 1,451, 1,424, 1,368, 1,267, 1,214, 1,148, 1,087, 1,033, 876, 857, and 817 cm^{-1} (Fig. 4(a)). The band at 1,710 cm^{-1} is attributed to the unconjugated C=O stretching vibration of carbonyl groups. The bands at 1,597 and 1,512 cm^{-1} arise from the aromatic skeletal vibrations. The 1,597 cm^{-1} band may be also contributed by a conjugated C=O vibration. The bands in the ranges of 1,480–1,400 and 900–800 cm^{-1} are due to the in-plane and out-plane C–H deformation vibrations on aromatic rings, respectively. The bands between 1,400 and 1,000 cm^{-1} are attributed to the C–C/C–O(H) vibrations. In particular, the band at 1,214 cm^{-1} is assigned to phenolic groups in lignin. As shown in the FTIR spectra of samples S2 (Fig. 4(b)) and S4 (Fig. 4(c)), the spectral changes due to Cr(III) reaction occurred at 1,710 cm^{-1}. The intensity of the 1,710 cm^{-1} band decreased as the corresponding bandwidth increased; the extent of both changes increased with increasing Cr(III) concentration. This downshift of the 1,710 cm^{-1} band indicated that the carbonyl groups are the binding sites for adsorbing Cr(III).

The carbonyl groups in lignin are associated with ketone, aldehyde, ester, quinone, and carboxyl functionalities [9]. Carboxyl groups have been suggested to be the metal binding sites of lignin [17–19]. If a carboxyl ligand is bound to a metal cation directly, the spectrum of the metal–carboxylate complex exhibits two bands (i.e. ν_a(COO) and ν_s(COO) vibrations) in the ranges of 1,700–1,500 and 1,400–1,200 cm^{-1},

Table 1
Structural parameters for Cr adsorbed on lignin after Cr(III) and Cr(VI) reactions obtained from Cr *K*-edge EXAFS analyses

Sample	Path	ΔE (eV)	CN[a]	R (Å)[b]	σ^2 (Å^2)[c]	ε ($\times10^{-3}$)[d]
Cr(III) reaction						
S4	Cr–O	0.41	6	1.99	0.003	0.98
Cr(VI) reaction						
S5	Cr–O	1.46	6	1.98	0.003	0.40
	Cr–C		1.1	2.40	0.005	
	Cr–C–O		2.2	3.09	0.005	
	Cr–Cr		0.46	2.98	0.003	
S6	Cr–O	0.89	6	1.98	0.003	0.25
	Cr–C		1.1	2.41	0.009	
	Cr–C–O		2.2	3.06	0.009	
	Cr–Cr		0.74	2.99	0.002	
S7	Cr–O	0.23	6	1.98	0.004	0.96
	Cr–C		1.2	2.42	0.008	
	Cr–C–O		2.4	3.00	0.008	
	Cr–Cr		0.90	2.99	0.004	

[a]CN: coordination number.
[b]*R*: interatomic distance.
[c]σ^2: Deby–Waller factor (disorder parameter).
[d]ε: error parameter, $\varepsilon = \sum(\chi_{exp} - \chi_{fit})^2 / \sum(\chi_{exp})^2$.

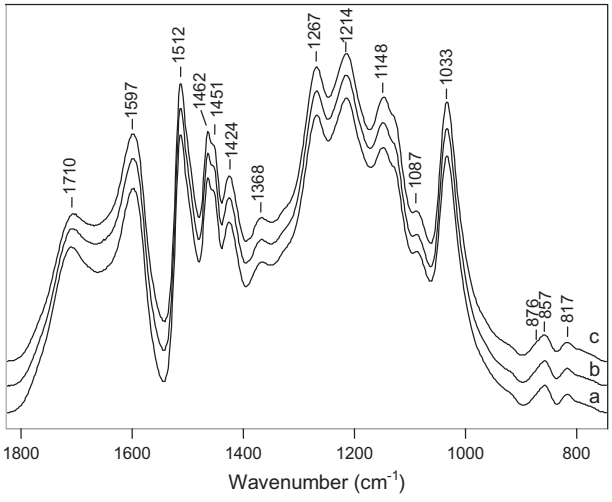

Fig. 4. FTIR spectra of lignin before (a) and after Cr(III) reaction (b and c). The samples (b) S2 and (c) S4 are indicated in Fig. 1.

respectively, depending on the carboxylate coordination [33]. Because the Cr(III) reaction did not cause any spectral changes in the region of 1,500–1,200 cm^{-1}, the occurrence of carboxylate complexes was ruled out. Thus, the downshift of the carbonyl bands is attributed to the increase in the C=O bond length, resulting from the interaction of the carbonyl groups with adsorbed Cr(III) (Fig. 5). Because of the polar character of the carbonyl group, the partial negative charge on the O end of the carbonyl bond can attract cationic species, such as $Cr(H_2O)_6^{3+}$. The carbonyl groups can interact with the hydration water of the adsorbed Cr(III) species through hydrogen bonding and/or with the central Cr^{3+} ion of the adsorbed Cr (III) through dipole–charge interaction (Fig. 5). These interactions withdraw electrons from the carbonyl bond and decrease the bond strength, consequently causing the observed increase of the C=O bond length and the downshift of the carbonyl stretching vibration (Fig. 4). On the basis of these results, the carbonyl

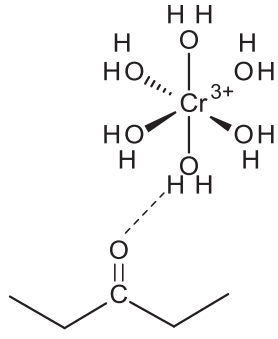

Fig. 5. The bonding mechanism of Cr(III) involves the formation of an outer-sphere complex between a $Cr(H_2O)_6^{3+}$ ion and a carbonyl group of lignin.

groups are determined to be the predominant sites for adsorbing Cr(III), which forms an outer-sphere complex on lignin surface (Fig. 5).

3.2. Cr(VI) reaction mechanism

Fig. 6 shows the amount of Cr(VI) removed by lignin as a function of the initial Cr(VI) concentration. When the initial Cr(VI) concentration was 204 mg L^{-1} or less, Cr(VI) was completely removed by lignin from the solution. At higher Cr(VI) concentrations, residual Cr(VI) in solution was observed. The removed Cr(VI) was converted to both Cr(III) in solution and Cr adsorbed on lignin (Fig. 6). Because Cr(III) was not originally present in the samples, its occurrence indicated the reduction of Cr(VI) to Cr(III) by lignin. Further clarification of the reaction mechanism necessitated the determinations of the oxidation state and bonding structure of Cr adsorbed on lignin after the reaction.

3.2.1. Cr K-edge XAS

In Fig. 7, the XANES spectra of samples S5–S7 (shown in Fig. 6) are compared with those of $Cr(VI)O_3$ and sample S4 obtained from the Cr(III) system. The XANES spectrum of Cr(VI) exhibited a strong pre-edge feature at $\Delta E = 4.0$ eV, which is attributed to the transition of 1s electrons to an unoccupied *p-d* hybridized orbital of Cr(VI) in tetrahedral coordination [34]. No apparent presence of this pre-edge feature in the XANES of samples S5 and S6 indicates that adsorbed Cr(VI) was completely converted to Cr(III). Although the pre-edge feature of Cr(VI) was observed in the XANES of sample S7, the weak intensity of this

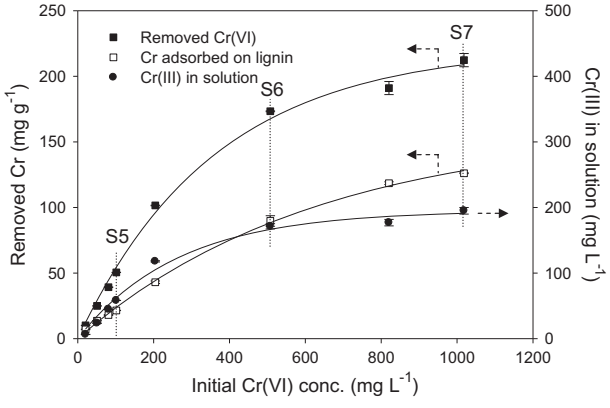

Fig. 6. Cr(VI) removal by lignin as a function of the initial Cr(VI) concentration at pH 2, and the consequent Cr adsorption on lignin and Cr(III) formation in solution.

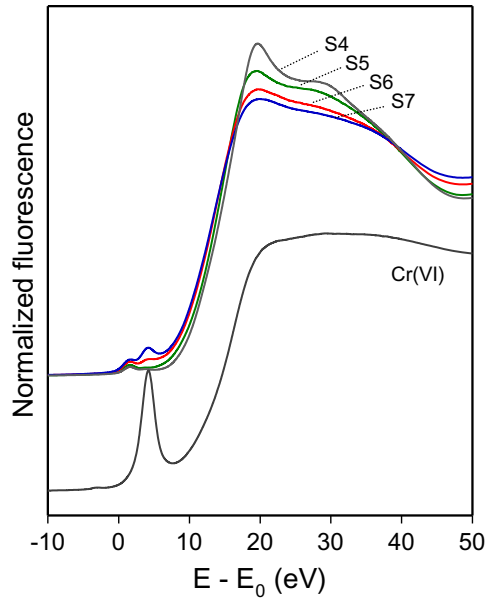

Fig. 7. Cr *K*-edge XANES for lignin reacted with Cr(VI) of different concentrations (samples S5–S7 are indicated in Fig. 6). The spectra of a Cr(VI) solution and sample S4 in Fig. 1 are shown for comparison.

feature indicated that only a trace amount of Cr(VI) remained in the sample (Fig. 7). Thus, the Cr adsorbed on lignin after Cr(VI) reaction was predominately Cr (III), irrespective of the initial Cr(VI) concentration used in this work. Because the oxidation states of Cr in solution and on lignin were both Cr(III), the reaction mechanism of Cr(VI) with lignin was solely a reductive transformation of Cr(VI) to Cr(III) on the lignin surface. The resultant Cr(III) was then either adsorbed on lignin or released back into the solution (Fig. 6).

Further investigation of the XANES spectra in Fig. 7 revealed that the spectra of samples S5–S7 obtained from Cr(VI) reaction were different from that of sample S4 from Cr(III) reaction. For example, the XANES spectrum of sample S5 exhibited a lower intensity of the white line and a broadening of the shoulder on the high-energy end of the white line compared with the spectrum of sample S4. These deviations became more significant with increasing amount of Cr(III) adsorbed due to Cr(VI) reaction (from S5 to S7 in Fig. 6). These spectral changes suggest that the electronic and coordination environments of Cr(III) adsorbed on lignin in the Cr(VI) system indeed differ from that in the Cr(III) system, which is similar to $Cr(H_2O)_6^{3+}$ species. Thus, non-aquo ligands may be present in the coordination environment of Cr (III) adsorbed on lignin due to Cr(VI) reduction.

The local structure of Cr(III) adsorbed on lignin was further investigated using EXAFS. Fig. 8 shows the experimental and fitted FT magnitudes derived from the EXAFS spectra of Cr adsorbed on samples S5–S7. Although these three spectra were quite similar, some differences were observed among their fitted parameters (Table 1). The strongest peak in the FT magnitude was attributed to the Cr(III)–O path (Fig. 8), and the corresponding CN and R were 6 and 1.98 Å, respectively (Table 1). No significant differences were observed among the fitted parameters of the Cr–O path obtained for different samples.

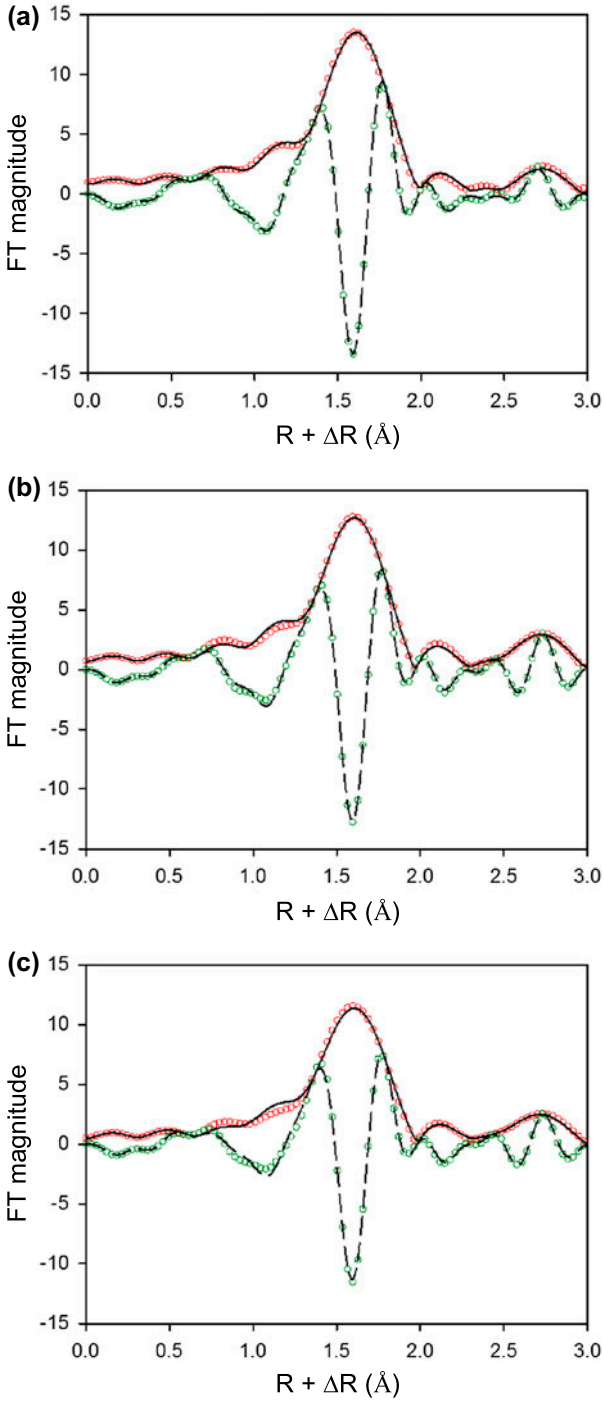

Fig. 8. Fourier transform magnitudes of the Cr K-edge EXAFS (solid line) and the corresponding imaginary part (dashed line) for lignin samples collected after Cr(VI) reaction. The samples (a) S5, (b) S6, and (c) S7 are indicated in Fig. 6. The open circles and lines represent the experimental and fitted data, respectively.

Small peaks between 2 and 3 Å in the FT magnitudes arose from FT ripples and/or scattering from C or Cr atoms around the central Cr^{3+} ion of the adsorbed Cr(III) species resulting from Cr(VI) reaction. Because the corresponding XANES spectra revealed the presence of a non-aquo ligand in the coordination environment of the Cr(III), the EXAFS spectra were first fitted using the theoretically derived parameters of the Cr–C and Cr–Cr paths. The CN of the Cr–C path was initially set to 1 or 2 to account for the monodentate and bidentate bonding configurations of surface complexes, respectively, with the functional groups of lignin. The inclusion of the Cr–Cr path was to account for the occurrence of hydrolytic Cr species. During the fitting process, inclusion of the multiple-scattering (MS) path related to the C shell was also observed to be necessary for improving the fits. Among different MS paths related to C with a value of $R < 3$ Å, the Cr–C–O path was selected because its amplitude was comparable to that of the single-scattering (SS) Cr–C path. An inherent limitation of including the MS path is the necessity to constrain the associated variables of the path to avoid over-parameterization with respect to the degree of freedom in the EXAFS spectra of the samples. Thus, the CN of the Cr–C–O path was set to be equal to twice that of the Cr–C path; the other parameters of the Cr–C–O path were constrained to those of the Cr–C path during the fitting process. The best fits for all the samples were obtained with the inclusion of both C and Cr shells around central Cr^{3+} in the adsorbed Cr(III) on lignin after Cr(VI) reaction. From S5 to S7, the amount of Cr adsorbed on lignin increased (Fig. 6). Correspondingly, the CN value of the Cr–Cr path increased from 0.5 to 0.9, whereas the CN and R values of the Cr–C paths and the R value of the Cr–Cr path were similar among the samples (Table 1).

The existence of C in the second shell of Cr suggests that an organic ligand is present in the coordination environment of Cr(III) adsorbed on lignin after Cr (VI) reaction. This observation is consistent with the information derived from the corresponding XANES spectra, indicating that non-aquo ligands are present in the coordination shell of the adsorbed Cr(III). The Cr–C distance of 2.39–2.42 Å implies that the Cr(III) is

bound to a functional group of lignin through inner-sphere complexation, although the type of functional group cannot be well deduced from the EXAFS results. Notably, unequivocal structural parameters are relatively difficult to obtain for a weak scatterer such as C when a strong scatterer such as Cr coexists in the same shell. Thus, the functional groups responsible for binding Cr(III) were determined on the basis of the complementary information provided by FTIR spectroscopy.

The presence of a Cr–Cr path with a distance of 2.98–2.99 Å was detected in the EXAFS spectra (Table 1). This Cr–Cr distance is consistent with that determined for the edge-sharing configuration of Cr octahedra, which contain double-hydroxo-bridge Cr–$(OH)_2$–Cr moieties, such as those in the structures of hydrolytic Cr species [28,35] and Cr-hydroxide precipitates [36,37]. In contrast, the Cr–Cr distance in the corner-sharing configuration of Cr octahedra is in the range of 3.85–3.88 Å [28], which is much longer than the Cr–Cr distance determined for the samples. Because the formation of a Cr-hydroxide precipitate is unlikely at low pH, this result is interpreted to indicate the formation of polynuclear Cr species such as dimer $[Cr_2(OH)_2(H_2O)_8]^{4+}$ and tetramer $[Cr_4(OH)_6(H_2O)_{12}]^{6+}$ [28,35]. The formation of dimers and tetramers results from the hydrolysis of Cr^{3+} ions in solution. They appear to be metastable due to slow equilibration [38] and are predominant in the pH range of 2–4 [28,35]. Because the reduction of Cr(VI) is accompanied by proton consumption, the concomitant elevation of local pH near the Cr(VI) reactive sites on lignin may lead to the hydrolysis of the resultant Cr (III) adsorbed on the surface. The increase in the CN value of the Cr–Cr path in the samples reacted with higher Cr(VI) concentrations (Table 1) is therefore attributable to the enhanced hydrolysis of Cr(III) resulting from Cr(VI) reduction.

3.2.2. FTIR spectroscopy

To determine the binding sites for adsorbing Cr (III) resulting from Cr(VI) reduction, FTIR spectra were obtained for lignin reacted with Cr(VI) at different concentrations and were compared with the spectrum of the original lignin (Fig. 9). The most noticeable differences due to Cr(VI) reaction are the decreasing intensities at 1,710 and 1,214 cm^{-1} and the increasing intensities at 1,650 and 1,387 cm^{-1} (Fig. 9). The bands at 1,710 and 1,214 cm^{-1} are assigned to carbonyl and phenolic groups, respectively; thus, the decreases of their intensities upon Cr(VI) reaction reveal that these two functional groups act as the

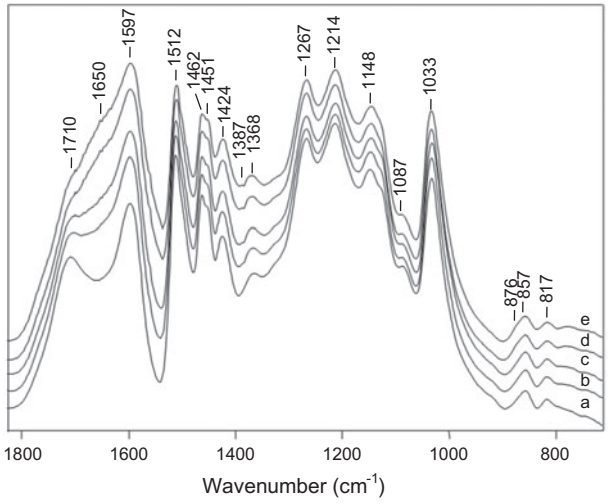

Fig. 9. FTIR spectra of lignin samples before (a) and after (b–e) Cr(VI) reaction. The initial Cr(VI) concentrations of the samples are (b) 50, (c) 102, (d) 508, and (e) 1,020 mg L^{-1}.

reductants for Cr(VI). New bands appeared at 1,650 and 1,387 cm^{-1}, which are assigned to the ν_a(COO) and ν_s(COO) vibrations of carboxyl groups, respectively. The appearance of these bands indicates that carboxyl groups formed on the lignin surface after Cr (VI) reaction. As suggested by Elovitz and Fish [39], the oxidation of phenols leads to the formation of quinones containing carbonyl groups. Further oxidation leads to the formation of carboxyl groups [39,40]. In the case of lignin, the oxidation of carbonyl and phenolic groups by Cr(VI) leads to the formation of carboxyl groups, as indicated by the increasing intensities of the bands at 1,650 and 1,387 cm^{-1}. The formation of quinonic groups as well as the adsorption of water onto oxidized lignin with an increasing content of carboxyl groups may also contribute to the increase of intensity of the broad band at 1,650 cm^{-1}.

The ν_a(COO) and ν_s(COO) bands at 1,650 and 1,387 cm^{-1}, respectively, indicate C_{2v} symmetry for the carboxyl groups [33]. Accordingly, the carboxyl groups may form bidentate or bridging complexes with Cr(III) (Fig. 10). The former has both oxygen atoms bound to the same Cr^{3+} ion, whereas the latter has each oxygen atom bound to a different Cr^{3+} ion (Fig. 10). These two chelating configurations cannot be distinguished on the basis of the positions of the ν_a(COO) and ν_s(COO) vibrations because the determination of their band positions was obscured by overlapping vibrational bands of other functional groups and adsorbed water (Fig. 9). To distinguish between both chelating configurations, the FTIR results were

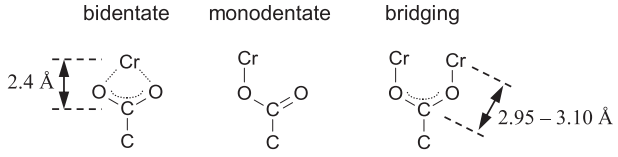

Fig. 10. Binding configurations of inner-sphere Cr^{3+}—carboxyl complexes (hydration water molecules of Cr^{3+} ion are omitted).

combined with the complementary information from the corresponding EXAFS spectra. As indicated in the EXAFS results, C is present in the second shell around Cr^{3+} in the adsorbed Cr(III). This observation, combined with the fact that the carboxyl groups chelate to Cr(III), indicates that the C in the second shell around Cr^{3+} is correlated to the carboxyl groups (Fig. 10). The Cr–C distances of adsorbed Cr(III) were determined to be 2.39–2.42 Å (Table 1), which were shorter than those (i.e. 2.95–3.10 Å) reported for Cr bound to one of the oxygen atoms of a carboxyl group, as in the monodentate or bridging configuration (Fig. 10) [26,41,42]. Moreover, the CN value of C was determined to be approximately one. Cr(III) resulting from Cr(VI) reduction is, therefore, concluded to be bound to one carboxyl group in the bidentate configuration.

Lignin has a high reduction capacity to convert Cr (VI) to Cr(III). In a redox reaction, the electron donor and acceptor must first form an inner- or outer-sphere complex to permit electron transfer between the redox couple [43]. Therefore, Cr(VI) must be bound to the functional groups of lignin before Cr(VI) can be reduced to Cr(III) by lignin. The reaction mechanism of Cr(VI) with lignin is therefore Cr(VI) adsorption and subsequent reduction. As revealed by the FTIR results, the carbonyl and phenolic groups of lignin are the predominant sites for reducing Cr(VI) to Cr(III). The high contents of these functional groups contribute the high Cr(VI) reduction capacity of lignin, resulting in the adsorbed Cr(VI) being almost completely reduced to Cr(III) on the lignin surface and only a trace amount of adsorbed Cr(VI) being detected on lignin at high Cr(VI) concentrations. A portion of the resultant Cr(III) is released back into solution, whereas the remaining part is chelated to the carboxyl groups resulting from the oxidation of carbonyl and phenolic groups by Cr(VI).

4. Conclusions

Cr *K*-edge XAS and FTIR spectroscopy provide complementary information for determining both the bonding structure of Cr on lignin after Cr(III) and Cr (VI) reactions and the corresponding reaction mechanisms. After Cr(III) reaction, Cr(III) is adsorbed onto the lignin surface with an octahedral structure similar to that of hydrated $Cr(H_2O)_6^{3+}$ ion. The results suggested that the adsorbed Cr(III) ions form outer-sphere complexes predominately with the carbonyl groups of lignin. The carbonyl groups may interact with the hydration water of the adsorbed Cr(III) species through hydrogen bonding and/or the central Cr^{3+} ion of the adsorbed Cr(III) through dipole–charge interaction. The reaction of Cr(VI) with lignin resulted in the reduction of Cr(VI) to Cr(III). Cr(VI) is first bound to the carbonyl and phenolic groups of lignin and is subsequently reduced to Cr(III), which is either adsorbed on the lignin surface or released back into solution. Simultaneously, the carbonyl and phenolic groups are oxidized by Cr(VI) to form carboxyl groups. According to the XAS and FTIR results, the adsorbed Cr(III) forms a bidentate inner-sphere complex with the carboxyl groups. The spectroscopic results of this study provide fundamental understanding of the reaction mechanisms of Cr(III) and Cr(VI) with lignin. This information can be further applied to understand the key role of lignin in determining the overall Cr(III) adsorption and Cr(VI) reduction by lignocellulosic materials.

Acknowledgment

The authors are grateful to Dr Jyh-Fu Lee and Dr Chi-Wen Bao for their assistances in XAS measurements. This work was financially supported by the National Science Council of Taiwan ROC under Project Nos. NSC97-2313-B-005-024-MY3 and NSC100-2628-B-002-005-MY3 and by the Ministry of Education of Taiwan ROC under the ATU plan. This research was carried out (in part) at the National Synchrotron Radiation Research Center in Hsinchu, Taiwan.

References

[1] J. Kotaś, Z. Stasicka, Chromium occurrence in the environment and methods of its speciation, Environ. Pollut. 107 (2000) 263–283.
[2] A.M. Zayed, N. Terry, Chromium in the environment: Factors affecting biological remediation, Plant Soil 249 (2003) 139–156.
[3] D. Mohan, C.U. Pittman, Activated carbons and low cost adsorbents for remediation of tri- and hexavalent chromium from water, J. Hazard. Mater. 137 (2006) 762–811.
[4] P. Miretzky, A.F. Cirelli, Cr(VI) and Cr(III) removal from aqueous solution by raw and modified lignocellulosic materials: A review, J. Hazard. Mater. 180 (2010) 1–19.

[5] B. Saha, C. Orvig, Biosorbents for hexavalent chromium elimination from industrial and municipal effluents, Coord. Chem. Rev. 254 (2010) 2959–2972.
[6] A.P. Lim, A.Z. Aris, A review on economically adsorbents on heavy metals removal in water and wastewater, Rev. Environ. Sci. Biotechnol. 13 (2014) 163–181.
[7] D.E. Kimbrough, Y. Cohen, A.M. Winer, L. Creelman, C. Mabuni, A critical assessment of chromium in the environment, Crit. Rev. Environ. Sci. Technol. 29 (1999) 1–46.
[8] H.W. Ma, M.L. Hung, P.C. Chen, A systemic health risk assessment for the chromium cycle in Taiwan, Environ. Int. 33 (2007) 206–218.
[9] L.B. Davin, N.G. Lewis, Lignin primary structures and dirigent sites, Curr. Opin. Biotechnol. 16 (2005) 407–415.
[10] T. Dizhbite, G. Zakis, A. Kizima, E. Lazareva, G. Rossinskaya, V. Jurkjane, G. Telysheva, U. Viesturs, Lignin—A useful bioresource for the production of sorption—Active materials, Bioresour. Technol. 67 (1999) 221–228.
[11] S. Babel, T.A. Kurniawan, Low-cost adsorbents for heavy metals uptake from contaminated water: A review, J. Hazard. Mater. 97 (2003) 219–243.
[12] Suhas, P.J.M. Carrott, M.M.L. Ribeiro Carrott, Lignin—From natural adsorbent to activated carbon: A review, Bioresour. Technol. 98 (2007) 2301–2312.
[13] Y.S. Shen, S.L. Wang, Y.M. Tzou, Y.Y. Yan, W.H. Kuan, Removal of hexavalent Cr by coconut coir and derived chars—The effect of surface functionality, Bioresour. Technol. 104 (2012) 165–172.
[14] S.L. Wang, J.F. Lee, Reaction mechanism of hexavalent chromium with cellulose, Chem. Eng. J. 174 (2011) 289–295.
[15] S.L. Wang, Y.C. Lin, Chromium(VI) Reactions of polysaccharide biopolymers, Chem. Eng. J. 181 (2011) 479–485.
[16] S.B. Lalvani, A. Hubner, T.S. Wiltowski, Chromium adsorption by lignin, Energy Sources 22 (2000) 45–56.
[17] A. Demirbaş, Adsorption of Cr(III) and Cr(VI) ions from aqueous solutions on to modified lignin, Energy Sources 27 (2005) 1449–1455.
[18] Y. Wu, S.Z. Zhang, X.Y. Guo, H.L. Huang, Adsorption of chromium(III) on lignin, Bioresour. Technol. 99 (2008) 7709–7715.
[19] A.B. Albadarin, A.H. Al-Muhtaseb, N.A. Al-laqtah, G.M. Walker, S.J. Allen, Biosorption of toxic chromium from aqueous phase by lignin: Mechanism, effect of other metal ions and salts, Chem. Eng. J. 169 (2011) 20–30.
[20] G.E. Brown Jr., J.G. Catalano, A.S. Templeton, T.P. Trainor, F. Farges, B.C. Bostick, T. Kendelewicz, C.S. Doyle, A.M. Spormann, K. Revill, G. Morin, F. Juillot, G. Calas, Environmental interfaces, heavy metals, microbes, and plants: Application of XAFS spectroscopy and related synchrotron radiation methods to environmental science, Phys. Scr. T115 (2005) 80–87.
[21] B.R. James, J.C. Petura, R.J. Vitale, G.R. Mussoline, Hexavalent chromium extraction from soils: A comparison of five methods, Environ. Sci. Technol. 29 (1995) 2377–2381.
[22] B. Ravel, M. Newville, ATHENA, ARTEMIS, HEPHAESTUS: Data analysis for X-ray absorption spectroscopy using IFEFFIT, J. Synchrotron Radiat. 12 (2005) 537–541.
[23] S.D. Kelly, D. Hesterberg, B. Ravel, Analysis of soils and minerals using x-ray absorption spectroscopy, in: A.L. Ulery, L.R. Drees (Eds.), Methods of Soil Analysis Part 5—Mineralogical Methods, Soil Science Society of America, Madison, WI, 2008, pp. 387–463.
[24] M. Newville, EXAFS analysis using FEFF and FEFFIT, J. Synchrotron Radiat. 8 (2001) 96–100.
[25] A.N. Christensen, P. Hansen, M.S. Lehmann, Isotope effects in the bonds of α-CrOOH and α-CrOOD, J. Solid State Chem. 21 (1977) 325–329.
[26] S.C. Chang, G.A. Jeffrey, The crystal structure of a basic chromium acetate compound, $[OCr_3(CH_3COO)_6{\cdot}3H_2O]^+ Cl^-{\cdot}6H_2O$, having feeble paramagnetism, Acta Crystallogr., Sect. B: Struct. Crystallogr. Cryst. Chem. 26 (1970) 673–683.
[27] D.C. Koningsberger, B.L. Mojet, G.E. van Dorssen, D.E. Ramaker, XAFS spectroscopy; funfamental principles and data analysis, Top. Catal. 10 (2000) 143–155.
[28] N. Torapava, A. Radkevich, D. Davydov, A. Titov, I. Persson, Composition and structure of polynulcear chromium(III) hydroxo complexes, Inorg. Chem. 48 (2009) 10383–10388.
[29] C. Hinz, Description of sorption data with isotherm equations, Geoderma 99 (2001) 225–243.
[30] L. Campbell, J.J. Rehr, G.K. Schenter, M.I. McCarthy, D. Dixon, XAFS Debye–Waller factors in aqueous Cr^{3+} from molecular dynamics, J. Synchrotron Radiat. 6 (1999) 310–312.
[31] M.I. Boyanov, K.M. Kemner, T. Shibata, B.A. Bunker, Local structure around Cr^{3+} ions in dilute acetate and perchlorate aqueous solutions, J. Phys. Chem. A 108 (2004) 5131–5138.
[32] H. Ohtaki, Ionic solvation in aqueous and nonaqueous solutions, Monatshefte fuer Chemie/Chemical Monthly 132 (2001) 1237–1268.
[33] G.B. Deacon, R.J. Phillips, Relationships between the carbon-oxygen stretching frequencies of carboxylato complexes and the type of carboxylate coordination, Coord. Chem. Rev. 33 (1980) 227–250.
[34] T. Yamamoto, Assignment of pre-edge peaks in K-edge x-ray absorption spectra of 3d transition metal compounds: Electric dipole or quadrupole? X-Ray Spectrom. 37 (2008) 572–584.
[35] L. Rao, Z. Zhang, J.I. Friese, B. Ritherdon, S.B. Clark, N.J. Hess, D. Rai, Oligomerization of chromium(III) and its impact on the oxidation of chromium(III) by hydrogen peroxide in alkaline solutions, J. Chem. Soc., Dalton Trans. (2002) 267–274.
[36] D. Rai, D.A. Moore, N.J. Hess, K.M. Rosso, L. Rao, S.M. Heald, Chromium(III) hydroxide solubility in the aqueous K^+–H^+–OH–CO_2–HCO_3–CO_3^{2-}–H_2O system: A thermodnyamic model, J. Solution Chem. 36 (2008) 1261–1285.
[37] J. Frommer, M. Nachtegaal, I. Czekaj, T.C. Weng, R. Kretzschmar, X-ray absorption and emission spectroscopy of Cr III (hydr)oxides: Analysis of the K-pre-edge region, J. Phys. Chem. A 113 (2009) 12171–12178.
[38] M. Henry, J.P. Jolivet, J. Livage, Aqueous chemistry of metal cations: Hydrolysis, condensation, and complexation, Struct. Bond. 77 (1992) 153–206.
[39] M.S. Elovitz, W. Fish, Redox interactions of Cr(VI) and substituted phenols: Products and mechanism, Environ. Sci. Technol. 29 (1995) 1933–1943.

[40] C.P. Rao, S.P. Kaiwar, Reduction of potassium chromate by d-fructose, d-galactose, d-mannose, d-glucose, and l-sorbose, Carbohydr. Res. 244 (1993) 15–25.
[41] H. Toftlund, O. Simonsen, E. Pedersen, Synthesis, characterization and structure of a new μ-acetato-di-μ-hydroxo bridged chromium(III) complex with a sexidentate binucleating pyridylamine ligand, Acta Chem. Scand. 44 (1990) 676–682.
[42] M. Eshel, A. Bino, Polynuclear chromium(III) carboxylates, Inorg. Chim. Acta 320 (2001) 127–132.
[43] K.M. Rosso, M. Dupuis, Electron transfer in environmental systems: A frontier for theoretical chemistry, Theor. Chem. Acc. 116 (2006) 124–136.